American Journal of Pathology, Vol. 160, No. 6, June 2002

Deficiency of Microvascular Thrombomodulin and Up-Regulation of Protease-Activated Receptor-1 in Irradiated Rat Intestine

Possible Link Between Endothelial Dysfunction and Chronic Radiation Fibrosis

Junru Wang,* Huaien Zheng,*‡ Xuemei Ou,* Louis M. Fink,‡ and Martin Hauer-Jensen*‡

From the Departments of Surgery and Pathology,‡ University of Arkansas for Medical Sciences and Central Arkansas Veterans Healthcare System, Little Rock, Arkansas*

Microvascular injury is believed to be mechanistically involved in radiation fibrosis, but direct molecular links between endothelial dysfunction and radiation fibrosis have not been established *in vivo*. We examined radiation-induced changes in endothelial thrombomodulin (TM) and protease-activated receptor-1 (PAR-1) in irradiated intestine, and their relationship to structural, cellular, and molecular aspects of radiation injury. Rat small intestine was locally exposed to fractionated X-radiation. Structural injury was assessed 24 hours and 2, 6, and 26 weeks after the last radiation fraction using quantitative histology and morphometry. TM, neutrophils, transforming growth factor-β, and collagens I and III were assessed by quantitative immunohistochemistry. PAR-1 protein was localized immunohistochemically, and cells expressing TM or PAR-1 transcript were identified by *in situ* hybridization. Steady-state PAR-1 mRNA levels in intestinal smooth muscle were determined using laser capture microdissection and competitive reverse transcriptase-polymerase chain reaction. Radiation caused a sustained, dose-dependent decrease in microvascular TM. The number of TM-positive vessels correlated with all parameters of radiation enteropathy and, after adjusting for radiation dose and observation time in a statistical model, remained independently associated with neutrophil infiltration, intestinal wall thickening, and collagen I accumulation. PAR-1 immunoreactivity and transcript increased in vascular and intestinal smooth muscle cells in irradiated intestine. PAR-1 mRNA increased twofold in irradiated intestinal smooth muscle. Intestinal irradiation up-regulates PAR-1 and causes a dose-dependent, sustained deficiency of microvascular TM that is independently associated with the severity of radiation toxicity. Interventions aimed at preserving or restoring endothelial TM or blocking PAR-1 should be explored as strategies to increase the therapeutic ratio in clinical radiation therapy. *(Am J Pathol 2002, 160:2063–2072)*

Intestinal toxicity (radiation enteropathy) is a major dose-limiting factor in radiation therapy of abdominal and pelvic tumors. Depending on the time of presentation relative to radiation therapy, radiation enteropathy is classified as acute or delayed. Acute radiation enteropathy is a result of epithelial barrier breakdown and mucosal inflammation. In contrast, delayed radiation enteropathy, which may present clinically many years after radiation therapy, is characterized by vascular sclerosis and progressive intestinal wall fibrosis. Microvascular injury is believed to be a key factor in the pathogenesis of radiation fibrosis in many organs, including intestine, and likely responsible for the chronic and progressive nature of delayed radiation injury. However, the mechanisms by which radiation causes endothelial dysfunction and how this contributes to the fibrogenic process are not yet known.

The transmembrane glycoprotein thrombomodulin (TM) is located on the luminal surface of endothelial cells and plays a pivotal role in maintaining the normal thrombohemorrhagic balance. Endothelial TM forms a complex with thrombin and thereby changes its substrate specificity. Thrombin, when bound to TM, no longer converts fibrinogen to fibrin or activates protease-activated receptor-1 (PAR-1), but instead activates protein C, a major anticoagulant and anti-inflammatory protein. The anticoagulant and anti-inflammatory properties of TM and activated protein C *in vivo* are well established in conditions

Supported by the National Institutes of Health (grant CA-83719) and the Central Arkansas Radiation Therapy Institute.

Accepted for publication March 5, 2002.

Address reprint requests to Martin Hauer-Jensen, M.D., Ph.D., Arkansas Cancer Research Center, 4301 West Markham, Slot 725, Little Rock, AR 72205. E-mail: mhjensen@life.uams.edu.

associated with generalized endothelial injury, as exemplified by a recent successful phase III trial with activated recombinant protein C in patients with severe sepsis.[1]

In contrast to conditions with generalized endothelial injury, the role of the TM-APC system in situations characterized by localized endothelial dysfunction and tissue fibrosis are less clear. However, recent clinical data point strongly to a role for TM in radiation-induced normal tissue toxicity.[2,3] Hence, although TM is abundantly expressed in the microvasculature of normal intestine, there is sustained deficiency of endothelial TM in intestines from patients who have received abdominal radiation therapy. We surmised that a local deficiency of endothelial TM after radiation causes insufficient activation of protein C and reduced scavenging of thrombin, thus enhancing the inflammatory, mitogenic, and fibrogenic effects of thrombin and contributing to the progression of intestinal wall fibrosis. The present study 1) examines dose- and time-dependent changes in TM in intestinal microvasculature in response to localized radiation therapy; 2) analyzes relationships between microvascular TM and structural, cellular, and molecular parameters of radiation toxicity; and 3) examines whether intestinal irradiation alters the expression of PAR-1, the primary mediator of thrombin's noncoagulant inflammatory, mitogenic, and fibrogenic functions.

Materials and Methods

Animals and Radiation Enteropathy Model

Forty-eight outbred male Sprague-Dawley rats (Harlan, Indianapolis, IN), procured at 43 to 49 days of age (175 to 200 g), were housed in conventional cages with free access to tap drinking water and standard rat chow (Formulab Chow 5008; Purina Mills, St. Louis, MO). A pathogen-free environment with controlled humidity, temperature, and 12-hour light-dark cycle was maintained. The experimental protocol was approved by the University of Arkansas for Medical Sciences Institutional Animal Care and Use Committee.

A surgical model for localized intestinal irradiation was used.[4,5] Briefly, rats were anesthetized, bilateral orchiectomy was performed, the internal inguinal ring was incised, and a loop of distal ileum was sutured to the inside of the empty scrotum. The resulting scrotal hernia contains a fixed 4-cm segment of small bowel that is accessible for fractionated irradiation (mimicking the clinical situation), without the need for additional surgery or risk of subsequent manipulation artifacts.[4,5] After irradiation, the intestine in the scrotal hernia develops structural, cellular, and molecular alterations similar to those seen clinically.

Irradiation was started after 3 weeks of postoperative recovery. The rats were anesthetized with methoxyflurane inhalation (Metofane; Pitman-Moore, Washington Crossing, NJ), and the scrotal hernia was exposed to localized fractionated irradiation as described in detail previously.[5,6] The 48 animals were randomly assigned to receive fractionated sham-irradiation ($n = 16$), 33.6 Gy in eight fractions ($n = 16$), or 67.2 Gy in 16 fractions ($n = 16$). Both sham-irradiation and the 4.2-Gy fractions were given daily without a weekend break. The two radiation doses were selected so as to produce minimal and moderate chronic radiation fibrosis, respectively.[5]

Quantitative Histology and Morphometry

Rats from each experimental group were euthanized 24 hours, 2 weeks, 6 weeks, or 26 weeks after the last irradiation, corresponding to the acute, subacute, intermediate, and chronic phases of radiation enteropathy in our model system. Irradiated or sham-irradiated intestines, as well as shielded intestine from each animal were procured. Specimens were fixed in methanol-Carnoy's solution for quantitative histopathology and immunohistochemistry, or in formalin for *in situ* hybridization and laser capture microdissection (LCM). The tissues were then processed routinely, paraffin-embedded, and sectioned at 4 to 5 μm (8 μm for LCM).

Structural injury was assessed using a validated radiation injury scoring system as described in detail and validated elsewhere.[4,7,8] Seven histopathological parameters of radiation injury (mucosal ulceration, epithelial atypia, thickening of subserosa, vascular sclerosis, intestinal wall fibrosis, ileitis cystica profunda, and lymph congestion) were assessed independently by two investigators in a blinded manner and graded (0 to 3) according to severity. Discrepancies in scores were resolved in conference. The sum of the scores for the individual alterations constitutes the radiation injury score. The radiation injury score is an indicator of the overall severity of radiation enteropathy, exhibits a consistent dose-response relationship, and correlates well with the incidence of delayed intestinal complications.

A decrease in the surface area of the intestinal mucosa is a sensitive parameter of both early and delayed radiation enteropathy. Mucosal surface area was estimated in vertical sections (sections cut perpendicular to the longitudinal axis of the gut) using a stereological projection/cycloid method as originally described by Baddeley and colleagues[9] and subsequently adapted to and validated in our model system.[8] Histological slides were projected onto a template of cycloids (a template of short curved lines in a systematic pattern). The number of intersections between cycloids and mucosal surface and the number of test points falling within the reference space (intestinal villi) were counted in five areas per specimen, selected according to a predefined grid pattern. The mean numbers of intersections and points were used to calculate the surface area corresponding to a 1-cm^3 mucosal reference volume (ie, surface/volume, cm^2/cm^3).

Intestinal wall thickness (from serosa to muscularis mucosae) correlates with the extent of connective tissue deposition after radiation. Five measurements per section, 500 μm apart, were obtained using an eyepiece linear microruler, averaged for each specimen, and used as a single value for statistical calculations.

Immunohistochemistry and Computer-Assisted Image Analysis

Quantitative immunohistochemistry and image analysis were used to determine 1) the number of submucosal TM-positive vessels; 2) neutrophil infiltration (myeloperoxidase as a marker); 3) collagen types I and III; and 4) extracellular matrix-associated transforming growth factor-β (TGF-β). PAR-1 immunoreactivity was assessed qualitatively.

Immunohistochemical staining was performed using the standard avidin-biotin complex technique, diaminobenzidine chromogen, and hematoxylin counterstaining. Appropriate positive and negative controls were included.

The primary antibodies, incubation times, and dilutions were: rabbit anti-rat TM antiserum (2 hours, 1:200 dilution; gift of Dr. Philip Majerus, Washington University School of Medicine, St. Louis, MO); polyclonal anti-myeloperoxidase antibody (1 hour, 1:100, A0398; DAKO, Carpinteria, CA); polyclonal antibodies against type I collagen (1310-01, 1:100 dilution; Southern Biotechnology Associates, Birmingham, AL) and type III collagen (1330-01, 1:100 dilution; Southern Biotechnology Associates); and polyclonal rabbit anti-TGF-β antibody (2 hours, 1:300 dilution, AB-100-NA; R&D, Minneapolis, MN). Additional verification of the TM staining pattern was performed using a new commercially available polyclonal rabbit anti-rat TM antibody (overnight, 1:100, ADI3380; American Diagnostica, Greenwich, CT). For PAR-1 staining, sections were incubated overnight with a polyclonal anti-rat PAR-1 antibody at 1:100 dilution (TR-R9; gift of Dr. Josiah Wilcox, Emory University, Atlanta, GA).

Quantitative assessment of immunoreactivity was performed using computerized image analysis (Image-Pro Plus; Media Cybernetics, Silver Spring, MD) as described in detail and validated previously.[2,3,10–12] TM-positive and -negative vessels in the intestinal submucosa were distinguished using color thresholding and counted in 20 fields per section.[2,3] The counts were restricted to vessels with diameters between 10 and 70 μm, as these vessels are consistently the most affected by radiation. Myeloperoxidase-positive cells were identified by color thresholding and counted in 10 fields per slide. Areas positive for collagen I or collagen III were measured according to Raviv and colleagues,[13] as adapted to our model system. Extracellular matrix-associated TGF-β immunoreactivity was measured as described and validated previously.[10,11,14]

In Situ *Hybridization*

Cellular sources of TM and PAR-1 in control and irradiated intestine were identified by *in situ* hybridization of formalin-fixed tissue sections.

Digoxigenin-labeled riboprobes for TM *in situ* hybridization were prepared as follows: a 1.7-kb segment of rat TM cDNA[15] was amplified by polymerase chain reaction (PCR) and inserted into the pGEM-T Easy Vector (Promega, Madison, WI). The plasmid was linearized with restriction endonucleases *Spe*I and *Sac*II for the sense and anti-sense probes, respectively. Digoxigenin-labeled sense and anti-sense cRNA probes were produced by *in vitro* transcription with T7 and SP6 RNA polymerases, using the DIG RNA-labeling kit (Roche Diagnostics, Indianapolis, IN). Probe labeling was evaluated with dot blot.

To generate the template for PAR-1 cRNA *in situ* hybridization probes, a 478-bp fragment within the coding region (572 to 1049 bp) was PCR-amplified from plasmid pSPORT1 that contained a 3814-bp insert including the entire coding region (51 to 1299 bp) and parts of the 5′- and 3′-untranslated regions of rat PAR-1 (Dr. Marschall Runge, University of North Carolina, Chapel Hill, NC). The amplified DNA fragment was subcloned into pGEM-T Easy Vector (Promega), to generate a new plasmid (oxPAR1c7). This plasmid was linearized with restriction enzymes *Spe*I and *Nco*I, respectively. Digoxigenin-labeled anti-sense and sense probes were generated using *in vitro* transcription with T7 and SP6 RNA polymerases, respectively, the DIG RNA-labeling kit (Roche Diagnostics), and dot blot for evaluation of probe labeling before *in situ* hybridization.

The same hybridization protocol was used to demonstrate cells expressing TM and PAR-1 transcripts. All chemicals and glassware were RNase-free during pre-

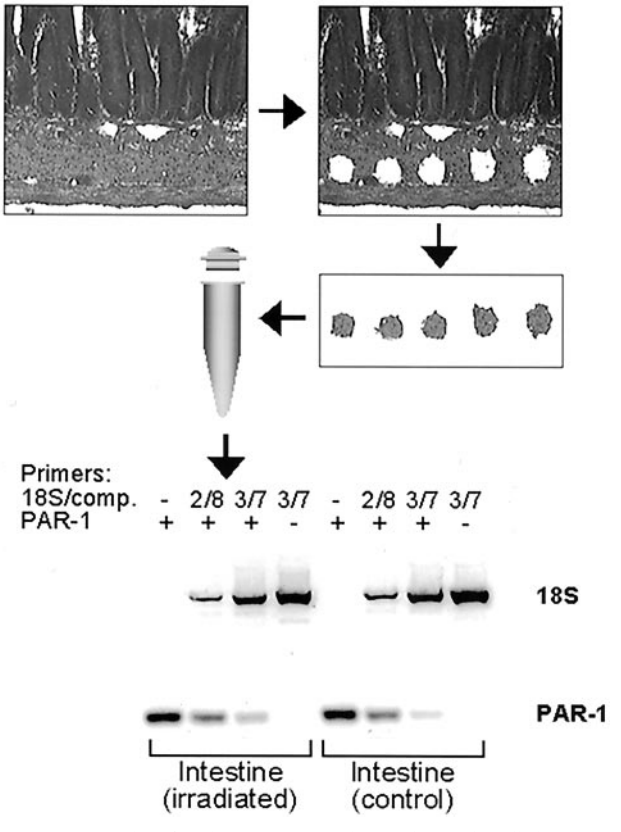

Figure 1. Procedure for obtaining intestinal smooth muscle cells by LCM. The figure shows (in sequence) a section of intestine before LCM, the same section after LCM (note the five holes in the smooth muscle cell layer), and an image of the LCM cap containing the microdissected smooth muscle samples. An example is also shown of the quantitative RT-PCR procedure used to assess steady-state PAR-1 mRNA levels using amplifying and attenuating primers for 18S RNA as reference (2/8 and 3/7 denotes the relative concentration of attenuating and amplifying 18S primers).

Table 1. Summary of Parameters Used to Assess the Intestinal Radiation Response (Median and Interquartile Range for Each Parameter, Experimental Group, and Time Point after the End of Irradiation)

	Sham-irradiated				4.2 Gy × 8	
	1 Day	2 Weeks	6 Weeks	26 Weeks	1 Day	2 Weeks
RIS	0 (0–1)	0 (0–0)	0 (0–1.5)	0 (0–0)	3 (2–3)	2 (0–2)
MSA	2.1 (2.0–2.2)	2.4 (2.3–2.5)	2.1 (2.1–2.2)	1.9 (1.8–2.0)	1.5 (1.1–1.7)	1.6 (1.5–1.9)
IWT	168 (151–238)	107 (105–120)	136 (128–158)	142 (98–167)	210 (173–289)	301 (290–409)
MPO	48 (36–57)	30 (21–60)	57 (43–69)	73 (36–97)	34 (34–63)	29 (27–36)
Coll1	13033 (12324–24180)	19366 (11422–29477)	22355 (9810–34425)	13290 (12270–30719)	19203 (6349–40328)	50035 (16355–70118)
Coll3	35377 (30854–36847)	37430 (32465–40563)	46152 (34324–48462)	27152 (25133–39907)	58941 (46619–73652)	79330 (74933–83066)
TGF-β	1807 (509–2625)	291 (165–344)	1213 (329–1468)	638 (448–1158)	37642 (10530–64856)	9660 (7696–17017)

RIS, radiation injury score; MSA, mucosal surface area (cm^2/cm^3); IWT, intestinal wall thickness (μm); MPO, number of myeloperoxidase-positive cells per 10 ×40 fields; Coll1, collagen I (μm^2); Coll3-collagen III (μm^2); TGF-β, extracellular matrix-associated transforming growth factor-β (μm^2). See text for further explanation of individual parameters. All parameters exhibit highly statistically significant radiation dose-dependent changes.

treatment and hybridization. The tissue sections were deparaffinized, rehydrated, and incubated with proteinase K (20 μg/ml) for 15 minutes at 37°C. The sections were then fixed in 4% paraformaldehyde for 10 minutes at 4°C, and rinsed in 0.1 mol/L triethanolamine-HCl (pH 8.0) for 1 minute, followed by 0.25% acetic anhydride in triethanolamine-HCl (pH 8.0) for 10 minutes. Sections were prehybridized with hybridization solution (Boehringer Mannheim, Indianapolis, IN) at 37°C for 30 minutes. Overnight hybridization was performed at 55°C in a 50% formamide-saturated humidified chamber. Sense probe and hybridization buffer without probe were used as negative controls. Sense and anti-sense probes, and anti-sense and nonprobe, respectively, were routinely applied to paired sections on the same slide. After hybridization, the sections were washed for 15 minutes at 40°C in 2× standard saline citrate (SSC) and 1× SSC, respectively, digested for 30 minutes at 37°C with 20 μg/ml of RNase A, and subsequently rinsed serially for 20 minutes in 2× SSC, 1× SSC, and 0.1× SSC at 37°C. Probe detection was conducted according to the instructions in the DIG Nucleic Acid Detection Kit (Boehringer Mannheim), and sections were counterstained lightly with methyl green or observed without counterstaining.

LCM and Multiplex Reverse Transcriptase (RT)-PCR

Steady state PAR-1 mRNA levels in intestinal smooth muscle from unirradiated and irradiated small bowel, 2 weeks after irradiation, were determined using LCM and semiquantitative RT-PCR analysis (Figure 1). Optimal conditions for the combined LCM-PCR procedure had been determined previously by comparing RNA yield from tissues fixed in different fixatives (neutral buffered formalin, methanol-Carnoy's solution, cryosections), RNA extracted using different reagents [Micro RNA Extraction Kit (Stratagene, La Jolla, CA), Trizol (Invitrogen, Carlsbad, CA), Paraffin Block RNA Isolation Kit (Ambion, Austin, TX)], with or without pretreatment of the tissue in RNAlater (Ambion) (data not shown), and the use of different housekeeping reference molecules (GAPDH, 18S).

Six- to eight-μm sections on uncharged and baked slides were freshly prepared from methanol-Carnoy's-fixed, paraffin-embedded tissue blocks. Slides were sequentially incubated in xylene (2 × 5 minutes), 100%, 95%, and 70% ethanol (1 × 5 minutes), briefly rinsed in diethyl pyrocarbonate-treated water, stained in hematoxylin for 10 seconds, and rinsed in diethyl pyrocarbonate-treated water until clear. Slides were then dehydrated in the ethanol and xylene, dried in a chemical hood, and stored in a desiccator until used. LCM was performed using the PixCell II LCM system (Arcturus, Mountain View, CA). Approximately 3000 spots per sample were captured on TFHS LCM caps (Arcturus) using a laser spot size 15 μm, power of 30 mW, and duration of 6 ms. RNA was subsequently extracted from the cap using the Micro RNA Extraction Kit (Stratagene) following the vendor's protocol, and dissolved in 30 μl of diethyl pyrocarbonate-treated water. The optional DNase treatment step during RNA extraction was essential for subsequent RT-PCR. The entire procedure was performed under RNase-free conditions.

Reverse transcription was performed using the SuperScript First-Strand Synthesis System (Invitrogen). Multiplex PCR was performed using the QuantumRNA Classic 18S Internal Standard kit (Ambion) following the vendor's protocol and rat PAR-1 primers in the same reaction. The cycle number was optimized by using a pooled sample in a series of PCR reactions (94°C, 30 seconds; 60°C, 30 seconds; 72°C, 30 seconds) that were terminated at every two cycles between 30 and 40 cycles. Subsequent PCR reactions were performed using the cycle number within the exponential amplification range.

To achieve reliable quantitation of the relatively low abundance PAR-1 mRNA (relative to 18S RNA), multiplex PCR was performed with a two to eight and a three to seven ratio of true 18S primers and competitors (ie, 18S primers that anneal to the template but do not result in amplification), to attenuate the 18S signal. Each reaction included samples of irradiated and unirradiated intestine from the same animal, ie, each animal provided its own control tissue. The PCR products were separated on 3% Metaphor agarose (BMA, Rockland, ME) in 1× Tris-borate-ethylenediaminetetraacetic acid buffer and stained with Gelstar (BMA). Bands were quantified using an image analysis system (AlphaImager 1220; Alpha Innotech, San Leandro, CA). The ratio between the PAR-1 band and the 18S band in each sample was calculated, and the amount of PAR-1 mRNA (relative to 18S)

Table 1. *Continued*

4.2 Gy × 8		4.2 Gy × 16			
6 Weeks	26 Weeks	1 Day	2 Weeks	6 Weeks	26 Weeks
1 (1–1)	0 (0–.75)	3 (3–5.25)	3 (.75–5.25)	6 (5–8.5)	5 (2–15)
1.5 (1.5–1.6)	1.7 (1.6–1.8)	1.3 (.9–1.5)	1.5 (1.5–1.7)	1.0 (.8–1.2)	1.5 (1.0–1.6)
241 (232–329)	219 (204–228)	380 (288–470)	354 (282–850)	758 (605–953)	524 (407–868)
51 (25–194)	70 (25–121)	119 (38–367)	177 (56–530)	689 (517–861)	130 (107–324)
42405 (12372–95459)	51427 (21679–63382)	41021 (29589–49586)	54682 (35467–78936)	58854 (31666–101304)	40549 (18297–78643)
102102 (94509–120522)	73739 (44644–123463)	62847 (53136–89131)	110090 (83369–136503)	99660 (60159–141901)	100986 (75774–132601)
7930 (4840–17451)	5525 (165–31131)	45753 (42691–88022)	11935 (7999–46397)	65667 (24016–116803)	66856 (1496–185198)

in irradiated intestine relative to unirradiated intestine for each animal was determined.

Statistical Methods

Sample size estimates were obtained using a software package for experimental design (PASS; NCSS, Kaysville, UT). The calculations were based on statistical power >80%, significance level 0.05, and the assumption of a difference in the number of TM-positive vessels between irradiated and unirradiated intestine (the primary endpoint of the present study) similar to what we had observed in our previous clinical studies.[2,3] Two-way analysis of variance (NCSS2000, NCSS) was to assess the effect of radiation dose and observation time on the number of TM-positive vessels and the various parameters of radiation enteropathy. Univariate associations between TM and the various endpoints were estimated using Spearman's rank correlation coefficient. Independent associations between the number of TM-positive vessels and parameters of radiation enteropathy (corrected for the influence of radiation dose and observation time) were assessed by regression analysis. Two-sided tests were used throughout for pairwise comparisons and P values <0.05 were considered statistically significant.

Results

Radiation Response

No animals died as a result of surgery or anesthesia. One animal from the 4.2 Gy × 16 group developed radiation-induced small bowel obstruction and was euthanized 19 days after completion of radiation therapy. There were no intestinal complications in the 4.2 Gy × 8 Gy group or among sham-irradiated animals.

Irradiated intestine exhibited dose-dependent changes consistent with previous experiments in our and other laboratories. Mucosal ulceration and inflammation were the predominant histological lesions during the early phase (1 day, 2 weeks) but were also present in some irradiated animals euthanized 6 weeks or 26 weeks after irradiation. In animals observed for 6 or 26 weeks after irradiation, there was prominent vascular sclerosis, as well as substantial reactive fibrotic thickening of subserosa and submucosa.

In accordance with the qualitative assessment, there were dose-dependent changes in radiation injury score ($P < 0.0001$), mucosal surface area ($P < 0.0001$), intestinal wall thickening ($P < 0.0001$), number of myeloperoxidase-positive cells ($P < 0.0001$), and in the immunoreactivity levels of extracellular matrix-associated TGF-β ($P = 0.0002$), collagen I ($P = 0.003$), and collagen III ($P < 0.0001$). These data are summarized in Table 1.

Thrombomodulin

Rat lung tissue used as positive control tissue for TM staining exhibited strong, well-defined immunoreactivity in the endothelium of alveolar capillaries and small vessels. There was no detectable immunoreactivity in negative control sections from lung or intestine, ie, when the primary antibody was omitted or substituted with nonimmune rabbit IgG. The TM antiserum and the commercial anti-rat TM antibody showed identical staining patterns in lung sections, as well as in irradiated and control intestine.

Representative sections demonstrating TM protein (immunohistochemistry) and TM transcript (*in situ* hybridization) in sham-irradiated and irradiated intestine are shown in Figure 2.

Sections from sham-irradiated intestine exhibited strong TM immunoreactivity in endothelium of capillaries, venules, and arterioles, with somewhat less prominent endothelial staining in larger arteries and veins. In contrast, irradiated intestine exhibited markedly reduced TM immunoreactivity in all types of vessels, and many were totally negative for TM, despite the obvious presence of endothelial cells.

In situ hybridization demonstrated TM transcript in endothelial cells, enteric neurons, and epithelial cells in control (unirradiated) intestine. Irradiated intestine showed unchanged TM hybridization signal in intestinal epithelium and neurons, but markedly decreased hybridization signal in endothelium of submucosal vessels at all observation times. Furthermore, although smooth muscle cells in control intestine were negative for TM transcript, smooth muscle cells and myofibroblasts in irradiated intestine exhibited strong hybridization signals, particularly in areas adjacent to radiation-induced mucosal ulcerations. These changes were most prominent during the early period after irradiation and less conspicuous at 26 weeks.

Image analysis of sham-irradiated intestinal specimens revealed that the proportion of TM-immunoreactive

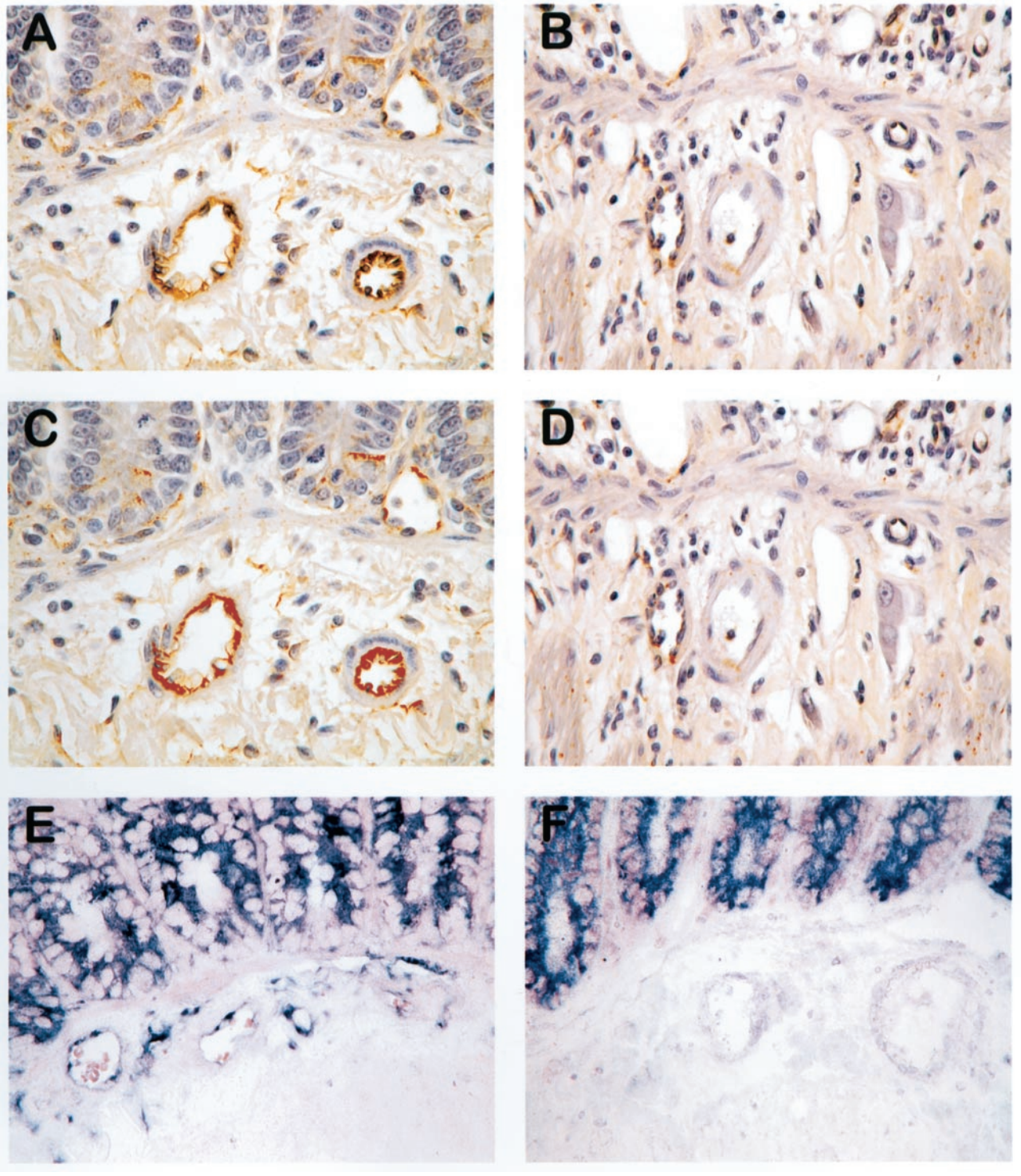

Figure 2. Unprocessed images demonstrating TM immunoreactivity in sham-irradiated (**A**) and irradiated (**B**) intestine; digitized images of sham-irradiated (**C**) and irradiated (**D**) intestine, thresholded (bright red color) for TM immunoreactivity; and TM transcript (dark blue/purple *in situ* hybridization signal) in sham-irradiated (**E**) and irradiated (**F**) intestine. Images obtained 2 weeks after irradiation (4.2 Gy × 16). Note prominent expression of TM in vascular endothelium of sham-irradiated intestine and minimal expression of endothelial TM in irradiated intestine. Original magnifications, ×400.

vessels was high (76 ± 2%, mean ± SE) and did not exhibit significant variation among time points ($P = 0.76$). Consistent with the qualitative results of TM staining, image analysis demonstrated a highly statistically significant dose-dependent decrease in the number of TM-positive vessels in irradiated intestine compared to sham-irradiated intestine ($P < 0.0001$). The number of TM-positive vessels in irradiated intestine decreased significantly throughout time ($P < 0.0001$), with most of the decrease occurring during the first 6 weeks after

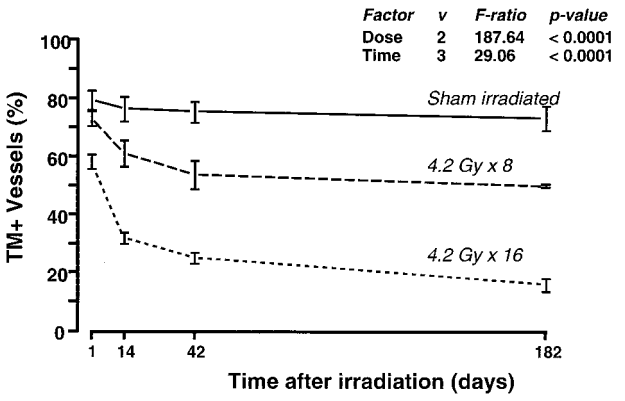

Figure 3. Relative number of TM-immunoreactive submucosal vessels in sham-irradiated and irradiated intestine, as determined by computer-assisted image analysis. Time-dependence and dose-dependence were highly statistically significant.

irradiation (Figure 3). For example, 1 day after the end of irradiation, the proportions of TM-positive vessels were 79 ± 3%, 73 ± 3%, and 58 ± 3% in the sham, 4.2 × 8 Gy and 4.2 × 16 Gy groups, respectively, whereas, in intestine procured 26 weeks after irradiation, the numbers were 75 ± 5%, 49 ± 1%, and 16 ± 3%.

Univariate analysis revealed significant correlations [Spearman's rho (ρ)] between the proportion of TM-positive vessels and all parameters used to assess radiation enteropathy: radiation injury score ($\rho = -0.60$, $P < 0.0001$), mucosal surface area ($\rho = 0.72$, $P < 0.0001$), intestinal wall thickness ($\rho = -0.80$, $P < 0.0001$), extracellular matrix-associated TGF-β immunoreactivity ($\rho = -0.57$, $P < 0.0001$), myeloperoxidase-positive cells ($\rho = -0.56$, $P = 0.0001$), collagen I immunoreactivity ($\rho = -0.67$, $P < 0.0001$), and collagen III immunoreactivity ($\rho = -0.72$, $P < 0.0001$). After adjusting for the effects of radiation dose and the influence of observation time after radiation in a multiple regression model, the decrease in number of TM-positive vessels remained independently associated with the number of myeloperoxidase-positive cells ($P = 0.02$), fibrotic thickening of the intestinal wall ($P = 0.0007$), and accumulation of collagen I ($P = 0.03$).

PAR-1

Representative images demonstrating localization of PAR-1 protein (immunohistochemistry) and transcript (*in situ* hybridization) in unirradiated and irradiated intestine are shown in Figure 4. Unirradiated intestine exhibited weak to moderate PAR-1 immunoreactivity in scattered inflammatory cells, vascular smooth muscle cells, and intestinal smooth muscle cells. There was increased PAR-1 immunoreactivity in most specimens of irradiated intestine, especially in vascular and smooth muscle cells in intestine procured up to 2 weeks after irradiation (Figure 4).

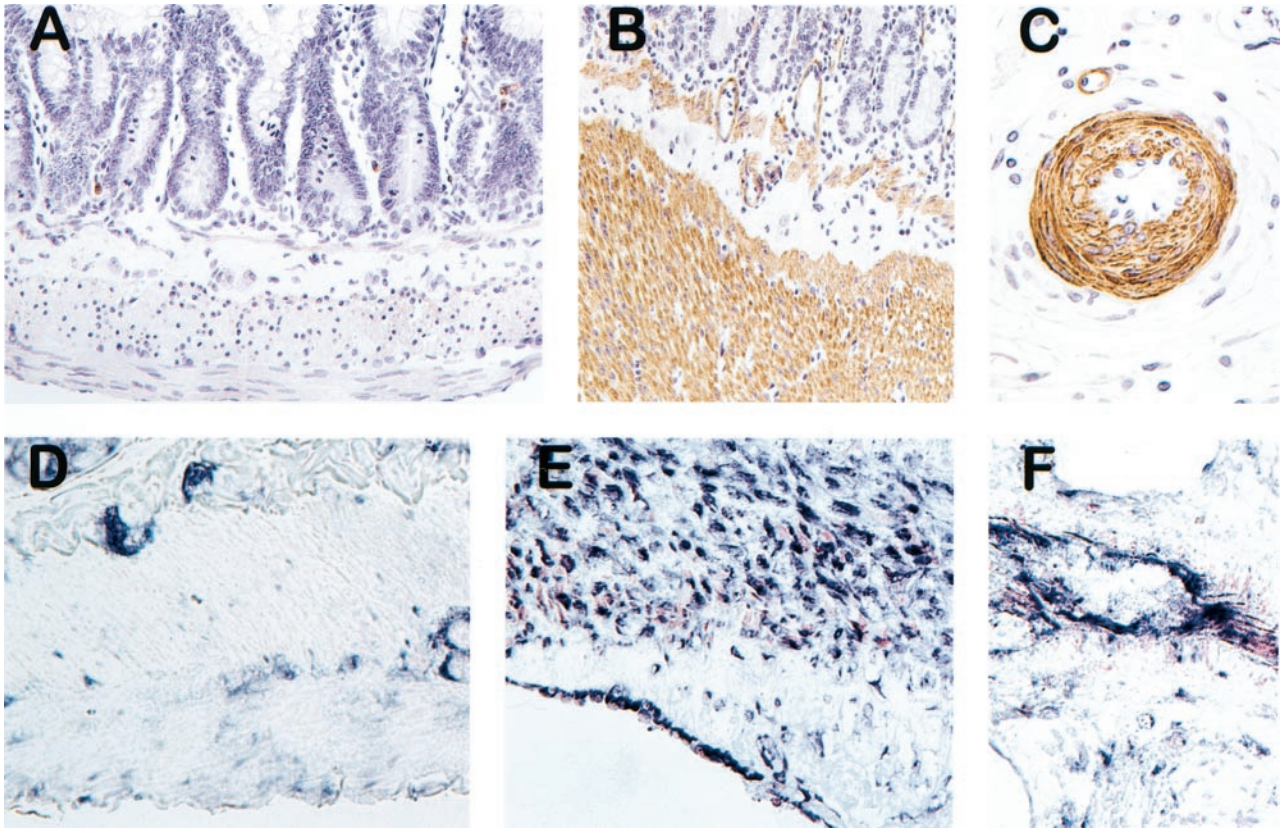

Figure 4. PAR-1 immunoreactivity in sham-irradiated (**A**) and irradiated (**B** and **C**) intestine; and PAR-1 transcript (*in situ* hybridization) in sham-irradiated (**D**) and irradiated (**E** and **F**) intestine. Images obtained 2 weeks after irradiation (4.2 Gy × 16). Note prominent increase in PAR-1 expression in intestinal smooth muscle cells and vascular wall after irradiation: in sham-irradiated intestine, intestinal smooth muscle cells exhibited weak PAR-1 immunoreactivity (**A**) and very little hybridization signal (**D**). In contrast, irradiated intestine exhibited strong PAR-1 immunoreactivity in intestinal (**B**) and vascular (**C**) smooth muscle cells and endothelium, as well as strong *in situ* hybridization signals in smooth muscle cells and endothelium (**E** and **F**). Original magnifications: ×200 (**A**, **B**, **D**, **E**); ×400 (**C**, **F**).

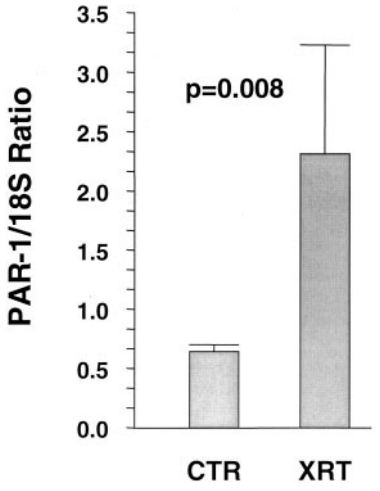

Figure 5. Steady-state PAR-1 mRNA levels in intestinal smooth muscle cells from unirradiated and irradiated intestine, obtained by LCM and multiplex RT-PCR. Values are expressed as mean (±SE) of relative expression levels (irradiated or sham-irradiated intestine relative to shielded intestine from the same animal).

The PAR-1 anti-sense probe showed specific hybridization with strong signals localized to the cellular cytoplasm. Sense probe and hybridization buffer without probe consistently showed minimal to no signal. Sham-irradiated intestine demonstrated PAR-1 transcript in epithelial cells (with no discernible difference along the crypt-villus axis), enteric neurons (Auerbach's plexus and Meissner's plexus), as well as weak signals in intestinal and vascular smooth muscle and endothelial cells. Intestinal tissue procured after irradiation, especially during the early period after radiation (1 day, 2 weeks), exhibited markedly increased hybridization signal in smooth muscle cells, endothelial cells, and mesothelial cells (Figure 4). Semiquantitative RT-PCR analysis of intestinal smooth muscle cells obtained from sections by LCM confirmed the *in situ* hybridization data, demonstrating a twofold increase in PAR-1 mRNA ($P = 0.008$, Figure 5).

Discussion

Vascular sclerosis was recognized as a prominent feature of delayed radiation fibrosis only 4 years after the discovery of the X-ray.[16] Radiation-induced vascular lesions are particularly prominent in small- to medium-sized blood vessels, and the high radiation sensitivity of vasculature is mainly linked to endothelial cells, a critical target cell for radiation injury.[17,18] Despite active research during the past several decades, direct molecular links between endothelial injury and radiation-induced tissue fibrosis have not been established *in vivo*.

There is ample evidence to suggest that radiation causes a state of local hypercoagulability. Hence, radiation induces a plethora of microvascular alterations, including endothelial cell swelling, increased permeability, interstitial fibrin deposition, and development of platelet-fibrin thrombi. At the cellular level, radiation causes increased apoptosis,[18,19] increased permeability,[20] inflammatory cell adhesion and emigration,[21,22] decreased fibrinolysis,[23] and increased prothrombotic properties by increased expression of tissue factor[24] and von Willebrand factor (vWF),[25] and decreased expression of prostacyclin[26] and TM.[27] These observations are consistent with the notion that radiation increases the prothrombotic properties of endothelial cells and that endothelial dysfunction may mediate, contribute to, or sustain some aspects of normal tissue radiation toxicity.

Correlative evidence from two clinical studies performed in our laboratory strongly suggest a role for TM in the pathogenesis of radiation fibrosis. First, in small bowel-resection specimens from patients undergoing operations for radiation enteropathy, there was a sixfold reduction in the number of TM-positive submucosal vessels compared to normal intestine (<15% *versus* >80%).[2] Second, analysis of specimens from patients who had received adjuvant radiation therapy before undergoing resection of rectal cancer revealed that the radiation-induced deficiency of microvascular TM was a premorbid phenomenon, ie, that TM was deficient before the development of discernible evidence of radiation enteropathy.[3] The deficiency of microvascular TM in irradiated intestine found in the present study is consistent with and of comparable magnitude to the findings in these clinical studies. Furthermore, the time- and radiation dose-dependence of the TM deficiency, as well as the statistically independent associations between decreased TM expression and hallmark features of radiation enteropathy also point to a role for TM in the pathogenesis of radiation enteropathy.

The mechanisms by which radiation causes TM deficiency is likely multifactorial. We have shown in a previous clinical study that although microvessels in irradiated intestine are deficient in TM, endothelial vWF immunoreactivity in these vessels is preserved.[2] Therefore, widespread loss of endothelial cell by apoptosis or other mechanisms (microvascular denudation) can essentially be ruled out as an explanation for the observed TM deficiency. The amount of TM present on the endothelial cell surface depends on the rate of synthesis, internalization, and release from the cell surface. Increased internalization is constitutive, does not seem to play an important role in other pathological states, and is unlikely to play a role in the present study.[28] Therefore, the two most plausible mechanisms by which radiation causes deficiency of endothelial TM are the increased release from the endothelial cell membrane into the circulation, and down-regulation at the gene level.

Although some release of TM from the endothelial membrane occurs in the normal situation, it is greatly enhanced during inflammation, for example by the combined action of TNF-α and neutrophils.[29] Cultured endothelial cells release TM into the medium as early as 6 hours after irradiation.[27] In contrast to the situation during systemic inflammation, however, the data regarding the effects of radiation therapy on the release of TM *in vivo* are sparse and inconclusive. Zhou and colleagues[30] found an overall increase in circulating TM levels in a heterogeneous cohort of patients undergoing radiation therapy of a variety of tumors in different parts of the body. In contrast, there was no evidence of increased circulating

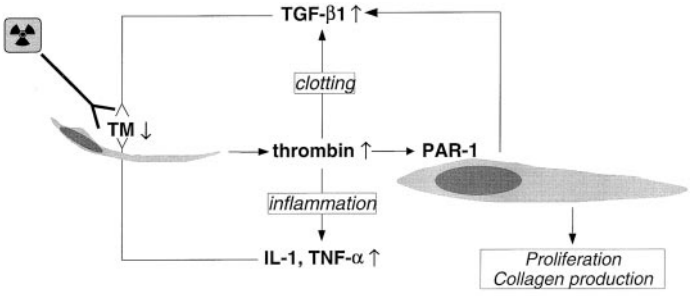

Figure 6. Proposed model linking radiation-induced endothelial dysfunction to subsequent vascular sclerosis and intestinal radiation fibrosis. Radiation causes TM deficiency in endothelial cells, leading to insufficient scavenging of locally formed thrombin, which exerts its procoagulant, pro-inflammatory, mitogenic, and profibrogenic effects on smooth muscle cells, fibroblasts, myofibroblasts, and other cell types in the irradiated tissue. Feed-back by cytokines sustains the endothelial TM deficiency and thus contributes to the chronicity of radiation injury.

TM in highly uniform groups of patients undergoing radiation therapy of lung cancer[31] or rectal cancer (KK Richter, personal communication). In fact, both of these studies showed moderately decreased circulating TM levels during radiation therapy.

The most likely explanation for the dramatic deficiency of endothelial cell TM in irradiated intestine observed in the present study is TM down-regulation. Interleukin-1 (IL-1), TNF-α, and TGF-β1, all of which are present at increased levels in radiation enteropathy and other situations with mucosal barrier breakdown and mucosal inflammation, render the endothelial cell surface procoagulant by up-regulating tissue factor and down-regulating TM.[32–37] The markedly reduced endothelial TM *in situ* hybridization signal in the microvasculature of irradiated intestine also points to down-regulation as the main reason for the local TM deficiency observed in our study. Interestingly, opposite to the observations in endothelial cells, intestinal smooth muscle cells in unirradiated intestine exhibited little or no TM transcript, whereas, TM was prominently expressed in intestinal smooth muscle from irradiated animals. Whether this up-regulation occurs in response to thrombin, as in vascular smooth muscle cells,[38] or by other mechanisms remains to be elucidated. Also, because TM immunoreactivity in irradiated intestinal smooth muscle remained low despite the presence of TM transcript, it is not clear whether the increased mRNA levels result in expression of TM protein on these cells and, if so, whether the protein is functional.

The robust radiation-induced up-regulation of PAR-1 observed in both vascular and intestinal smooth muscle cells suggests that PAR-1 may be implicated in radiation-induced vascular sclerosis as well as in radiation fibrosis of the intestinal wall. Hence, postradiation endothelial TM deficiency may result in insufficient local scavenging of thrombin, thus enhancing thrombin's procoagulant effects, as well as its pro-inflammatory, profibrogenic, and promitogenic effects mediated by the proteolytic activation of PAR-1 on endothelial, smooth muscle, and other cells.

The mechanism of PAR-1 up-regulation may be a direct effect of radiation, as well as an indirect effect of the subsequent inflammatory process. Hence, the regulation of PAR-1 is redox-sensitive,[39] and up-regulation in endothelial and mesenchymal cells has been demonstrated in other inflammatory and fibrotic conditions.[40] PAR-1 expression is also induced in skeletal muscle cells by exposure to IL-1, TNF-α, or TGF-β,[41] and in smooth muscle by angiotensin II.[42] The striking increase in the expression of PAR-1 in irradiated intestinal smooth muscle cells, as demonstrated in the present study by immunohistochemistry, *in situ* hybridization, and RT-PCR analysis, may be mechanistically important. In the intestine, smooth muscle cells are the predominant producers of collagen in many pathological states, including radiation enteropathy. Radiation causes a marked increase in the normally very low proliferation rate of smooth muscle cells and strongly induces their expression of TGF-β1 and collagens I and III.[12,43] Taken together, our observations that microvascular endothelium in irradiated intestine is deficient of TM, whereas there is increased postradiation expression of PAR-1 by intestinal smooth muscle are compatible with the notion that smooth muscle cells are important effectors in radiation fibrosis, and that mitogenic, profibrogenic, and pro-inflammatory effects of thrombin play a role in the mechanisms of radiation-induced fibrosis and vascular sclerosis. The finding that TM deficiency is independently associated with features of early radiation toxicity (inflammation), as well as delayed radiation toxicity (fibrosis) further supports this model, depicted schematically in Figure 6. It is tempting to speculate that some of these mechanisms may also apply to other types of tissue injury, and that PAR-1 may play roles in other postinjury tissue-remodeling processes.

In conclusion, this study demonstrates that localized fractionated irradiation of the intestine causes a consistent, time-dependent, dose-dependent decrease in TM on microvascular endothelium, and that the severity of TM deficiency correlates with structural, cellular, and molecular aspects of early and delayed radiation toxicity. Irradiated intestine also exhibits striking up-regulation of PAR-1 in intestinal smooth muscle cells in the proximity of areas of severe radiation injury. These findings corroborate and extend our previous clinical studies. They also suggest that deficient scavenging of thrombin and subsequent activation of PAR-1 on intestinal smooth muscle cells may be important factors in radiation enteropathy and possibly represent the molecular link between endothelial dysfunction and radiation fibrosis. Future studies should address the clinically important possibilities that preserving or restoring endothelial TM or blocking PAR-1 may protect against normal tissue toxicity in patients undergoing radiation therapy of cancer.

References

1. Bernard GR, Vincent J-L, Laterre P-F, LaRosa SP, Dhainaut J-F, Lopez-Rodriguez A, Steingrub JS, Garber GE, Helterbrand JD, Ely W, Fisher CJ: Efficacy and safety of recombinant human activated protein C for severe sepsis. N Engl J Med 2001, 344:699–709

2. Richter KK, Fink LM, Hughes BM, Sung C-C, Hauer-Jensen M: Is the loss of endothelial thrombomodulin involved in the mechanism of chronicity in late radiation enteropathy? Radiother Oncol 1997, 44:65–71
3. Richter KK, Fink LM, Hughes BM, Shmaysani HM, Sung C-C, Hauer-Jensen M: Differential effect of radiation on endothelial cell function in rectal cancer and normal rectum. Am J Surg 1998, 176:642–647
4. Hauer-Jensen M, Poulakos L, Osborne JW: Effects of accelerated fractionation on radiation injury of the small intestine: a new rat model. Int J Radiat Oncol Biol Phys 1988, 14:1205–1212
5. Langberg CW, Sauer T, Reitan JB, Hauer-Jensen M: Tolerance of rat small intestine to localized single dose and fractionated irradiation. Acta Oncol 1992, 31:781–787
6. Langberg CW, Waldron JA, Baker ML, Hauer-Jensen M: Significance of overall treatment time for the development of radiation-induced intestinal complications. An experimental study in the rat. Cancer 1994, 73:2663–2668
7. Hauer-Jensen M, Sauer T, Devik F, Nygaard K: Late changes following single dose roentgen irradiation of rat small intestine. Acta Radiol Oncol 1983, 22:299–303
8. Langberg CW, Sauer T, Reitan JB, Hauer-Jensen M: Relationship between intestinal fibrosis and histopathologic and morphometric changes in consequential and late radiation enteropathy. Acta Oncol 1996, 35:81–87
9. Baddeley AJ, Gundersen HJG, Cruz-Orive LM: Estimation of surface area from vertical sections. J Microsc 1986, 142:259–276
10. Richter KK, Langberg CW, Sung C-C, Hauer-Jensen M: Increased transforming growth factor β (TGF-β) immunoreactivity is independently associated with chronic injury in both consequential and primary radiation enteropathy. Int J Radiat Oncol Biol Phys 1997, 39:187–195
11. Richter KK, Sung C-C, Langberg CW, Hauer-Jensen M: Association of transforming growth factor β (TGF-β) immunoreactivity with specific histopathologic lesions in subacute and chronic experimental radiation enteropathy. Radiother Oncol 1996, 39:243–251
12. Wang J, Zheng H, Sung C-C, Richter KK, Hauer-Jensen M: Cellular sources of transforming growth factor β (TGF-β) isoforms in early and chronic radiation enteropathy. Am J Pathol 1998, 153:1531–1540
13. Raviv G, Kiss R, Vanegas JP, Petein M, Danguy A, Schulman C, Wespes E: Objective measurement of the different collagen types in the corpus cavernosum of potent and impotent men: an immunohistochemical staining with computerized-image analysis. World J Urol 1997, 15:50–55
14. Hauer-Jensen M, Richter KK, Wang J, Abe E, Sung C-C, Hardin JW: Changes in transforming growth factor β1 (TGF-β1) gene expression and immunoreactivity levels during development of chronic radiation enteropathy. Radiat Res 1998, 150:673–680
15. Wang J, Yao A, Wang J-Y, Sung C-C, Fink LM, Hardin JW, Hauer-Jensen M: cDNA cloning and sequencing, gene expression, and immunolocalization of thrombomodulin in the Sprague-Dawley rat. DNA Res 1999, 6:57–62
16. Gassmann A: Zur Histologie der Röntgenulcera. Fortschr a d Geb d Roentgenstr 1899, 2:199–207
17. Fajardo LF: The unique physiology of endothelial cells and its implication in radiobiology. Radiation Tolerance of Normal Tissues. Edited by JM Vaeth, JL Meyer. Front Ther Oncol. Basel, Karger, 1989, pp 96–112
18. Paris F, Fuks Z, Kang A, Capodieci P, Juan G, Ehleiter D, Haimovitz-Friedman A, Cordon-Cardo C, Kolesnick R: Endothelial apoptosis as the primary lesion initiating intestinal radiation damage in mice. Science 2001, 293:293–297
19. Langley RE, Bump EA, Quartuccio SG, Medeiros D, Braunhut SJ: Radiation-induced apoptosis in microvascular endothelial cells. Br J Cancer 1997, 75:666–672
20. Law MP: Vascular permeability and late radiation fibrosis in mouse lung. Radiat Res 1985, 103:60–76
21. Dunn MM, Drab EA, Rubin DB: Effects of irradiation on endothelial cell-polymorphonuclear leukocyte interactions. J Appl Physiol 1986, 60:1932–1937
22. Hallahan D, Clark ET, Kuchibhotla J, Gewertz BL, Collins T: E-selectin gene induction by ionizing radiation is independent of cytokine induction. Biochem Biophys Res Commun 1995, 217:784–795
23. Svanberg L, Åstedt B, Kullander S: On radiation-decreased fibrinolytic activity of vessel walls. Acta Obstet Gynecol Scand 1976, 55:49–51
24. Verheij M, Dewit LGH, van Mourik JA: The effect of ionizing radiation on endothelial tissue factor activity and its cellular localization. Thromb Haemost 1995, 73:894–895
25. Jahroudi N, Ardekani AM, Greenberger JS: Ionizing radiation increases transcription of the von Willebrand factor gene in endothelial cells. Blood 1996, 88:3801–3814
26. Rubin DB, Drab EA, Ts'ao C, Gardner D, Ward WF: Prostacyclin synthesis in irradiated endothelial cells cultured from bovine aorta. J Appl Physiol 1985, 58:592–597
27. Zhou Q, Zhao Y, Li P, Bai X, Ruan C: Thrombomodulin as a marker of radiation-induced endothelial cell injury. Radiat Res 1992, 131:285–289
28. Teasdale MS, Bird CH, Bird P: Internalization of the anticoagulant thrombomodulin is constitutive and does not require a signal in the cytoplasmic domain. Immunol Cell Biol 1994, 72:480–488
29. Boehme MWJ, Deng Y, Raeth U, Bierhaus A, Ziegler R, Stremmel W, Nawroth PP: Release of thrombomodulin from endothelial cells by concerted action of TNF-α and neutrophils: in vivo and in vitro studies. Immunology 1996, 87:134–140
30. Zhou Q, Zhao Y, Xu C, Yu Z, Yao D, Gao Y, Ruan C: Increase in plasma thrombomodulin and decrease in plasma von Willebrand factor after regular radiotherapy of patients with cancer. Thromb Res 1992, 68:109–118
31. Hauer-Jensen M, Kong F-M, Fink LM, Anscher MS: Circulating thrombomodulin during radiation therapy of lung cancer. Radiat Oncol Invest 1999, 7:238–242
32. Nawroth PP, Handley DA, Esmon CT, Stern DM: Interleukin 1 induces endothelial cell procoagulant while suppressing cell-surface anticoagulant activity. Proc Natl Acad Sci USA 1986, 83:3460–3464
33. Archipoff G, Beretz A, Freyssinet J, Klein-Soyer C, Brisson C, Cazenave J: Heterogeneous regulation of constitutive thrombomodulin or inducible tissue-factor activities on the surface of human saphenous-vein endothelial cells in culture following stimulation by interleukin-1, tumor necrosis factor, thrombin or phorbol ester. Biochem J 1991, 273:679–684
34. Scarpati E, Sadler JE: Regulation of endothelial cell coagulant properties: modulation of tissue factor, plasminogen activator inhibitors, and thrombomodulin by 12-myristate 13-acetate and tumor necrosis factor. J Biol Chem 1989, 264:20705–20713
35. Lentz SR, Tsiang M, Sadler JE: Regulation of thrombomodulin by tumor necrosis factor-α: comparison of transcriptional and posttranscriptional mechanisms. Blood 1991, 77:542–550
36. Ohji T, Urano H, Shirahata A, Yamagishi M, Higashi K, Gotoh S, Karasaki Y: Transforming growth factor beta1 and beta2 induce down-modulation of thrombomodulin in human umbilical vein endothelial cells. Thromb Haemost 1995, 73:812–818
37. Ranganathan G, Blatti SP, Subramaniam M, Fass DN, Maihle NJ, Getz MJ: Cloning of murine tissue factor and regulation of gene expression by transforming growth factor type beta 1. J Biol Chem 1991, 266:496–501
38. Ma S-F, Garcia JGN, Reuning U, Little SP, Bang NU, Dixon EP: Thrombin induces thrombomodulin mRNA expression via the proteolytically activated thrombin receptor in cultured bovine smooth muscle cells. J Lab Clin Med 1997, 129:611–619
39. Capers Q, Laursen JB, Fukui T, Rajagopalan S, Mori I, Lou P, Freeman BA, Berrington WR, Griendling KK, Harrison DG, Runge MS, Alexander RW, Taylor WR: Vascular thrombin receptor regulation in hypertensive rats. Circ Res 1997, 80:838–844
40. Marra F, DeFranco R, Grappone C, Milani S, Pinzani M, Pellegrini G, Laffi G, Gentilini P: Expression of the thrombin receptor in human liver: up-regulation during acute and chronic injury. Hepatology 1998, 27:462–471
41. Mbebi C, Rohn T, Doyenette M-A, Chevessier F, Jandrot-Perrus M, Hantai D, Verdiere-Sahuque M: Thrombin receptor induction by injury-related factors in human skeletal muscle cells. Exp Cell Res 2001, 263:77–87
42. Fisslthaler B, Schini-Kerth VB, Fleming I, Busse R: Thrombin receptor expression is increased by angiotensin II in cultured and native vascular smooth muscle cells. Cardiovasc Res 1998, 38:263–271
43. Wang J, Zheng H, Hauer-Jensen M: Influence of short-term octreotide administration on chronic tissue injury, transforming growth factor β (TGF-β) overexpression, and collagen accumulation in irradiated rat intestine. J Pharmacol Exp Ther 2001, 297:35–42